

Distance Is All You Need: Radial Dispersion for Uncertainty Estimation in Large Language Models

Manh Nguyen*, Sunil Gupta, Hung Le
Applied Artificial Intelligence Initiative
Deakin University, Australia

Abstract

Detecting uncertainty in large language models (LLMs) is essential for building reliable systems, yet many existing approaches are overly complex and depend on brittle semantic clustering or access to model internals. We introduce **Radial Dispersion Score (RDS)**, a simple, training-free, fully model-agnostic uncertainty metric that measures the radial dispersion of sampled generations in embedding space. Specifically, given N sampled generations embedded on the unit hypersphere, RDS computes the total ℓ_1 distance from the empirical centroid, i.e., the mean embedding, providing a direct geometric signal of semantic variability. A lightweight probability-weighted variant further incorporates the model’s own token probabilities when available, outperforming nine recent state-of-the-art baselines. Moreover, RDS naturally extends to effective per-sample uncertainty estimates that complement probability- and consistency-based methods while remaining lightweight for practical use. Across four challenging free-form question-answering datasets and four LLMs, our metrics achieve state-of-the-art hallucination detection and best-of- N performance, while remaining robust and scalable with respect to sample size and embedding choice. These results highlight the practical value of RDS and its contribution toward improving the trustworthiness of LLMs.

1 Introduction

Large language models (LLMs) exhibit remarkable reasoning and generation capabilities, yet they frequently produce *hallucinations*, fluent but factually incorrect or unsubstantiated outputs (Ji et al., 2023; Huang et al., 2025). Detecting when a language model is uncertain remains essential for building reliable, trustworthy systems. Among existing approaches, uncertainty estimation is one of the most effective tools for hallucination detection.

*Corresponding author: manh.nguyen@deakin.edu.au

†Code: <https://github.com/manhitv/RDS>

Predictive entropy is the information-theoretic gold standard for quantifying uncertainty (Malinin and Gales, 2021), but exact computation is infeasible due to the exponential output space. As a result, recent work relies on Monte Carlo sampling. For example, semantic entropy (Kuhn et al., 2023a; Farquhar et al., 2024) and its extensions (Lin et al., 2023; Nikitin et al., 2024) cluster sampled responses in an external embedding space and compute entropy over semantic equivalence classes. While effective, these methods suffer from two critical drawbacks: (i) accurate semantic clustering is inherently brittle, i.e., a single response can belong to multiple plausible clusters, and (ii) by operating exclusively on the *generation* space, they discard the LLM’s own probability estimates and thus ignore a rich source of epistemic uncertainty directly available from the model itself. More recently, Nguyen et al. (2025) utilised these probabilities by introducing PRO, an approximation of predictive entropy using only the top- K generation probabilities derived from negative log-likelihood. Although effective on open-weight models, PRO remains model-specific, requires a calibration set to select the optimal K , and cannot be applied to black-box LLMs.

A parallel line of research approximates differential entropy through geometric properties of hidden representations. EigenScore (Chen et al., 2024) uses the trace of the covariance matrix (equivalently, the sum of its eigenvalues) of LLM internal states as a lightweight proxy. While computationally attractive, EigenScore is fundamentally *model-specific* because internal states are inaccessible for black-box LLMs and even for some open-weight models. In addition, it saturates in high-uncertainty regimes, mapping a wide range of highly uncertain cases to the same maximal value and thus reducing sensitivity, especially when the output distribution exhibits antipodal modes (see Figure 1).

To tackle these problems, we propose **Radial**

Dispersion Score (RDS), a simple, training-free, and model-agnostic uncertainty metric with a clean geometric interpretation. RDS avoids semantic clustering, does not access hidden states, and requires no calibration or model internals. Given N sampled generations embedded on the unit hypersphere using an external encoder, RDS is defined as the total ℓ_1 radial dispersion from the empirical centroid (the mean embedding). Intuitively, it directly quantifies the aggregate angular spread of output generations: the larger the sum of distances from the centroid, the greater the overall semantic dispersion. Theoretically, RDS lower-bounds the trace of the embedding covariance matrix and thus preserves a monotonic connection to the differential entropy of the (unknown) continuous output distribution. Unlike EigenScore, it remains highly discriminative in high-entropy, opposing-cluster regimes.

We further introduce a probability-weighted variant, RDS_w , which incorporates LLM token-level probabilities when available, thereby emphasizing the actual structure of the model’s predictive distribution. This weighting preserves meaningful directional distinctions and shifts the centroid toward high-probability generations, yielding a more faithful estimate of the representative embedding. Geometrically, RDS_w is exactly the 1-Wasserstein distance between the empirical distribution of generations and its barycenter, providing a geometric foundation for its stability and sensitivity. RDS applies uniformly to both black-box and open-weight models, while RDS_w is available for models exposing token-level probabilities. We also highlight that RDS naturally supports per-sample uncertainty scoring, which is crucial for applications such as best-of- N selection and confidence-based filtering. Unlike aggregated metrics such as semantic entropy, which are defined at the set level and require additional heuristics to assign scores to individual samples, RDS admits a natural per-sample uncertainty score based on each sample’s radial deviation from the centroid. In summary, our contributions are threefold:

- We introduce RDS and RDS_w , a family of simple, parameter-free, model-agnostic uncertainty estimators grounded in radial dispersion geometry, supported by formal theoretical analyses.
- We show that RDS naturally yields strong, lightweight per-sample uncertainty estimates

suitable for practical use.

- Across four free-form QA datasets, four diverse LLMs, and both hallucination detection and best-of- N evaluations, our metrics deliver state-of-the-art performance and demonstrate strong robustness and scalability.

2 Related Work

Uncertainty Estimation for LLMs Uncertainty estimation methods for LLMs can be grouped into three main families. (1) *Probability-based methods* include (average) negative log-likelihood remain surprisingly competitive (Guerreiro et al., 2023; Manakul et al., 2023). PRO (Nguyen et al., 2025) recently improved upon these by approximating predictive entropy using only the top- K generation probabilities and an adaptive threshold to filter noisy samples. While effective on open-weight models, these approaches cannot be used with black-box APIs and often require calibration data. (2) *Semantic entropy and its extensions* (Kuhn et al., 2023a; Farquhar et al., 2024; Lin et al., 2023; Nikitin et al., 2024; Qiu and Miikkulainen, 2024) cluster sampled responses in an external embedding space and compute entropy over clusters’ entropy (or density). Despite strong performance, they inherit the brittleness of clustering and discard the LLM’s own probability signal. (3) *Geometric methods* such as EigenScore (Chen et al., 2024), use the covariance trace as a fast entropy proxy but require internal states and saturate in high-uncertainty regimes such as antipodal distributions. Geometric Volume (Phillips et al., 2025) is model-agnostic via convex-hull of archetypes but computationally heavy due to non-convex archetypal analysis and poor scaling of hull computation. Parallel work explores multi-model uncertainty via Jensen–Shannon divergence (Kruse et al., 2025), and hidden-state Monte-Carlo sampling (Gao et al., 2025). Our method belongs to none of these families: it is geometric yet model-agnostic, leverages generation probabilities only optionally, and avoids clustering entirely, and is provably more sensitive than trace-based metrics.

Best-Of- N Metric Best-of- N samples N candidates and picks the highest-likelihood or highest-quality one (Wang et al., 2022). Universal and fine-grained self-consistency (Chen et al., 2023; Wang et al., 2024) extend this idea but remain limited for open-ended generation because they require ad-

ditional LLM calls to evaluate or refine samples. Self-certainty (Kang et al., 2025) addresses this by leveraging a sample’s output probability distribution to estimate response quality. Our method is complementary to these approaches: it operates directly in the embedding space, imposes no additional test-time compute, and requires no extra generations, and connects naturally to uncertainty estimation through its geometric formulation.

3 Preliminaries

From Discrete to Continuous Entropy The information-theoretic gold standard for predictive uncertainty is the conditional entropy of the output distribution:

$$H(Y|x) = - \sum_y p(y|x) \log p(y|x) \quad (1)$$

where Y is the (discrete) output random variable, x is the input. A low predictive entropy indicates a sharply concentrated output distribution, whereas a high value indicates more diverse outputs.

Differential entropy is the continuous analogue of this quantity, obtained by replacing discrete probabilities with a density $f(y|x)$. In the context of LLMs, such a density is induced by embedding sampled completions using either internal hidden states or an external encoder. Approximating the conditional distribution of embedding vectors as Gaussian $Y|x \sim \mathcal{N}(\mu, \Sigma)$ yields a closed-form differential entropy (Zhouyin and Liu, 2021):

$$\begin{aligned} H_{\text{de}}(Y|x) &= \frac{1}{2} \log \det(\Sigma) + \frac{d}{2} (\log 2\pi + 1) \quad (2) \\ &= \frac{1}{2} \sum_{i=1}^d \log \lambda_i + C, \quad (3) \end{aligned}$$

where λ_i are the eigenvalues of Σ , d is the embedding dimension, and C is an additive constant.

EigenScore as a Practical Proxy While differential entropy provides a principled measure, computing it requires estimating the full covariance matrix eigenspectrum. Chen et al. (2024) introduces a computationally simple surrogate for differential entropy: the *EigenScore*, defined as the trace of the covariance of the hidden representations:

$$\text{EigenScore}(X) = \text{tr}(\Sigma) \quad (4)$$

$$= \frac{1}{N} \sum_{i=1}^N \|\mathbf{u}_i - \bar{\mathbf{u}}\|_2^2 \quad (5)$$

$$= \sum_{i=1}^N \lambda_i \propto H_{\text{de}}(X), \quad (6)$$

where \mathbf{u}_i denotes the embedding of the i -th sampled completion and $\bar{\mathbf{u}} = \frac{1}{N} \sum_{i=1}^N \mathbf{u}_i$ is the sample mean embedding. EigenScore equals the average squared ℓ_2 distance from the centroid: it approaches 0 when embeddings collapse (low uncertainty) and increases with isotropic spread (high uncertainty).

4 Methodology

4.1 Uncertainty Estimation via Radial Dispersion Score

To estimate the uncertainty of an LLM’s output given a prompt x , we leverage the geometry of semantic embeddings sampled from the model’s generations. Specifically, we generate N ($N > 1$) sequences $\{y_1, y_2, \dots, y_N\}$ conditioned on x using multinomial sampling. Each generation is embedded via an encoder \mathbf{E} and then explicitly ℓ_2 -normalized to obtain unit-norm vectors $\mathbf{u}_i \in \mathbb{R}^d$:

$$\mathbf{u}_i = \frac{\mathbf{E}(y_i)}{\|\mathbf{E}(y_i)\|_2}, \quad \|\mathbf{u}_i\|_2 = 1. \quad (7)$$

These embeddings represent points on the unit hypersphere, where proximity reflects semantic similarity among output generations. High uncertainty manifests as dispersed embeddings (diverse plausible outputs), while low uncertainty yields clustered embeddings (Kuhn et al., 2023b). We quantify this dispersion simply using the ℓ_1 -norm dispersion from the centroid, termed Radial Dispersion Score (RDS), which is defined as:

$$\text{RDS}(x) = \sum_{i=1}^N \|\mathbf{u}_i - \bar{\mathbf{u}}\|_1. \quad (8)$$

where $\bar{\mathbf{u}} = \frac{1}{N} \sum_{i=1}^N \mathbf{u}_i$ denotes the empirical centroid of the sampled embeddings. Intuitively, RDS measures the total radial dispersion of each embedding from the centroid, with larger values indicating greater dispersion and, consequently, higher uncertainty, vice versa.

We choose the ℓ_1 -norm over the ℓ_2 -norm for two reasons: (1) it provides a tighter upper bound on

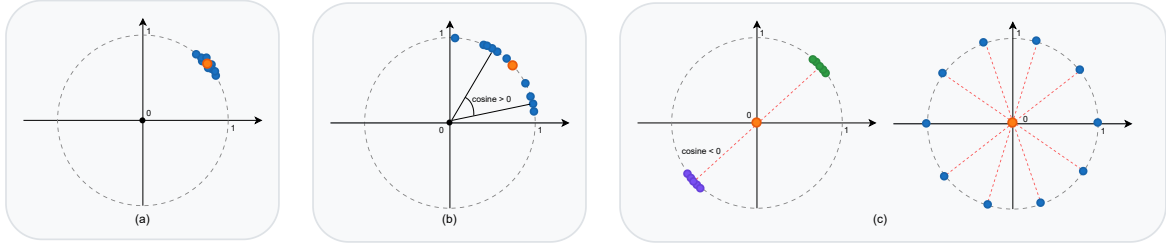


Figure 1: RDS vs. EigenEmbed across three uncertainty regimes illustrated using ten unit-norm 2D embeddings. Orange circles denote the empirical centroid (mean vector). (a) Low uncertainty: all generations collapse into a tight semantic cluster; $\text{RDS} \approx \text{EigenEmbed} \approx 0$. (b) Hemispheric spread: embeddings are broadly dispersed but remain positively aligned with the mean (all cosines with the centroid > 0); Both metrics indicate moderate-to-high uncertainty ($\text{RDS} \approx \sqrt{N}$, $\text{EigenEmbed} \approx 0.8\text{--}0.9$). (c) Opposing-cluster regime: two or more tight clusters with negative inter-cluster cosines cancel the mean vector toward zero, causing EigenEmbed to saturate near 1 despite growing structural disagreement, whereas RDS scales with the magnitude of these opposing directions ($\geq \sqrt{N}$), making it substantially more sensitive and diagnostically useful for detecting high-uncertainty generations.

variance-based measures (as formalized in Proposition 1, Section 4.2), and (2) it responds more strongly to large deviations in the embedding space (Hastie et al., 2005), making extreme dispersion easier to detect.

Probability-Weighted Variant Geometric dispersion alone overlooks variation in generation likelihoods. Prompt ambiguity, task difficulty, or knowledge gaps can make some outputs far more probable than others (Kuhn et al., 2023a; Hou et al., 2024), while generation probabilities have been shown to correlate with correctness (Kadavath et al., 2022). To incorporate this, we define a *probability-weighted* variant that emphasizes dispersion among high-probability outputs while reducing the impact of low-probability, potentially noisy generations (Nguyen et al., 2025). Let $p_i = p(y_i|x) / \sum_j p(y_j|x)$ denote the normalized generation likelihood of each sequence, the weighted RDS at the prompt level is then defined as:

$$\text{RDS}_w(x) = \sum_{i=1}^N p_i \|\mathbf{u}_i - \bar{\mathbf{u}}_w\|_1, \quad \bar{\mathbf{u}}_w = \sum_{i=1}^N p_i \mathbf{u}_i. \quad (9)$$

Here, the probability of each generation $p(y_i|x)$ is estimated empirically by Average Negative Log-Likelihood (ANLL) (Manakul et al., 2023), which is widely used in prior work (Aichberger et al., 2024; Nguyen et al., 2025).

Beyond its geometric simplicity, **RDS is inherently robust and broadly applicable**: it relies solely on generated outputs rather than LLM internal states, operates in a lower-dimensional embed-

ding space, and avoids model-specific architectural assumptions. This makes RDS easy to compute, lightweight in practice, and compatible with any black-box LLM. Weighted RDS further refines this signal when generation probabilities are available (e.g., grey-box or open-weight models), yielding a more faithful estimate of uncertainty by prioritizing dispersion among high-probability outputs.

4.2 Theoretical Analysis

In this section, we analyze the theoretical properties of RDS and its weighted variant, RDS_w .

4.2.1 RDS Connection to EigenScore

To begin, we introduce **EigenEmbed**, defined as EigenScore computed from an *external encoder* \mathbf{E} rather than LLM internal hidden states. This allows fair comparison with RDS, which also operates on external embeddings. Figure 1 illustrates a 2D geometric intuition comparing RDS and EigenEmbed using ten unit-norm embeddings. In the coherent (a) and hemispheric-spread (b) regimes, both metrics agree. The most critical divergence occurs in the opposing-cluster regime (Figure 1c), a prevalent failure mode in which LLMs produce overconfident yet contradictory generations. Here, multiple tight semantic clusters lie in roughly opposite directions on the hypersphere, resulting in a strong cancellation of the mean vector. As a result, EigenEmbed rapidly saturates and loses discriminative power, whereas RDS continues to scale with the true angular separation. We formalize this discrepancy below.

Proposition 1. Let $\{\mathbf{u}_i\}_{i=1}^N \subset \mathbb{R}^d$ be unit-norm embeddings ($\|\mathbf{u}_i\|_2 = 1$). Let the centered embeddings be $\mathbf{v}_i = \mathbf{u}_i - \bar{\mathbf{u}}$. Then:

(1) $\text{EigenEmbed} = \frac{1}{N} \sum_{i=1}^N \|\mathbf{v}_i\|_2^2 \in [0, 1]$.

(2) $\text{RDS} \geq \text{EigenEmbed}$.

Equality in (2) holds if and only if all \mathbf{u}_i are identical. The gap becomes larger as $\bar{\mathbf{u}} \rightarrow \mathbf{0}$.

Proof. See Appendix A.1. \square

This parameter-free lower bound is tight for any $d \geq 1$ and $N \geq 2$.

Extremal Case: $\bar{\mathbf{u}} = \mathbf{0}$. When the centroid is at zero, the embeddings form a perfectly *balanced* configuration around the origin (Figure 1c), giving $\mathbf{v}_i = \mathbf{u}_i$. EigenEmbed then attains its maximum:

$$\text{EigenEmbed} = \frac{1}{N} \sum_{i=1}^N \|\mathbf{u}_i\|_2^2 = 1.$$

For RDS, non-negativity of $\|\mathbf{v}_i\|_1 \forall i$ yields

$$\text{RDS} = \sum_{i=1}^N \|\mathbf{v}_i\|_1 \geq \sqrt{\sum_{i=1}^N \|\mathbf{v}_i\|_2^2} = \sqrt{N}.$$

Thus, the two metrics diverge sharply in this regime, with RDS remaining responsive to the extent of semantic dispersion. Moreover, a zero centroid imposes further structural constraints on the embeddings as follows.

Proposition 2. If the embeddings satisfy $\bar{\mathbf{u}} = \mathbf{0}$, then the average pairwise cosine similarity is

$$\frac{1}{N(N-1)} \sum_{i \neq j} \mathbf{u}_i^\top \mathbf{u}_j = -\frac{1}{N-1} < 0. \quad (10)$$

Consequently, for every i , there exists at least one $j \neq i$ such that $\mathbf{u}_i^\top \mathbf{u}_j < 0$.

Proof. See Appendix A.2. \square

This negative-average structure is a *geometric signature of semantic disagreement*: sampled generations are not merely diverse but actively opposed, forming antipodal or multi-cluster cancellation regimes, an explicit signature of semantic diversity and uncertainty. Such geometric configurations highlight regimes of maximal uncertainty, independent of the specific choice of dispersion metric.

4.2.2 RDS_w Connection to Optimal Transport

The weighted RDS_w coincides exactly with the 1-Wasserstein distance (Earth Mover’s Distance) between the discrete probability measure

$$\mu = \sum_{i=1}^N p_i \delta_{\mathbf{u}_i} \in \mathcal{P}(\mathbb{R}^d)$$

and the Dirac measure at its own barycenter

$$\nu = \delta_{\bar{\mathbf{u}}_w}, \quad \bar{\mathbf{u}}_w = \sum_{i=1}^N p_i \mathbf{u}_i,$$

when the ground cost is $c(\mathbf{a}, \mathbf{b}) = \|\mathbf{a} - \mathbf{b}\|_1$.

Because the target measure ν consists of a single Dirac mass, every feasible coupling must send the entire mass p_i located at \mathbf{u}_i directly to $\bar{\mathbf{u}}_w$. Hence, the coupling set $\Pi(\mu, \nu)$ contains a single deterministic plan, yielding the closed form:

$$W_1(\mu, \nu) = \sum_{i=1}^N p_i \|\mathbf{u}_i - \bar{\mathbf{u}}_w\|_1 = \text{RDS}_w(x)$$

(Santambrogio, 2015; Peyré et al., 2019).

This closed-form expression makes RDS_w computationally trivial (no optimization required), while inheriting the geometric meaning and theoretical properties of the 1-Wasserstein distance.

4.3 Per-Sample Uncertainty Metrics

A distinctive advantage of RDS is its natural extensibility to per-sample uncertainty scoring, allowing us to assign an individual uncertainty estimate to each generated sequence y_i , enabling powerful applications such as best-of- N selection and confidence-based filtering. We define the per-sample variants as:

$$\text{RDS}^s(y_i) = \|\mathbf{u}_i - \bar{\mathbf{u}}\|_1, \quad (11)$$

$$\text{RDS}_w^s(y_i) = \|\mathbf{u}_i - \bar{\mathbf{u}}_w\|_1, \quad (12)$$

where $\bar{\mathbf{u}}$ and $\bar{\mathbf{u}}_w$ are the (weighted) centroids introduced in Eq. (8) and Eq. (9), respectively. These scores measure the ℓ_1 -distance of each embedding, corresponding to an individual generated sequence y_i , from the centroid of the sampled distribution.

The intuition aligns closely with the principle underlying self-consistency (Wang et al., 2022): generations that represent majority or high-probability answers tend to cluster tightly around the centroid and thus receive low per-sample scores, whereas

outliers or rare answers are pushed farther away and obtain higher scores. The weighted variant RDS_w^s is particularly powerful because the centroid \bar{u}_w is shifted toward high-probability generations. Consequently, low-probability or semantically deviant outputs are penalized more heavily, yielding a per-sample score that correlates better with generation correctness and model confidence. By explicitly capturing the underlying goal of the sampling process, which is to identify the most representative semantic signals, these per-sample metrics provide stable and informative uncertainty estimates that complement probability-based and consistency-based approaches, while remaining lightweight for practical use.

5 Experimental Results

5.1 Experiment Setup

Datasets We use four established benchmarks covering scientific QA and mathematical reasoning: (1) Scientific QA: SciQ (Welbl et al., 2017), and GPQA Diamond (GPQA) (Rein et al., 2024), (2) Mathematical reasoning: Arithmetics (Brown et al., 2020), and SVAMP (Patel et al., 2021). All benchmarks are experimented over full test sets. We provide the links to these datasets in Table 5, Appendix A.4.

Models We evaluate on four popular instruction-tuned open-weight models from distinct families: Falcon3-7B (Almazrouei et al., 2023), Gemma2-9B (Mesnard et al., 2024), Llama3.1-8B, and Llama3.2-3B (Grattafiori et al., 2024). We refer to them as Falcon3, Gemma2, Llama3.1, and Llama3.2.

Baselines For *hallucination detection* tasks (Section 5.2), we compare our method against nine established uncertainty estimators: (1) Average Log Likelihood (ANLL) (Guerreiro et al., 2023), (2) Negative Log Likelihood (NLL) (Aichberger et al., 2024), (3) PRO (Nguyen et al., 2025), (4) Semantic Entropy (SE) (Kuhn et al., 2023a), (5) Degree (Deg) (Lin et al., 2023), (6) Semantic Density (SD) (Qiu and Miikkulainen, 2024), (7) Self Consistency (SC) (Wang et al., 2022), (8) EigenScore (ES) (Chen et al., 2024), and (9) EigenEmbed (EE), which is EigenScore computed on external embeddings. For *best-of-N* setting (Section 5.3), we consider only methods that yield a directly comparable per-sample score; set-level methods such as SE, Deg, SD, and EE inherently depend on clustering or ag-

gregation and are therefore excluded. Instead, we additionally include the recent Self-Certainty (CE) baseline (Kang et al., 2025).

Evaluation Protocol Following Kuhn et al. (2023a); Qiu and Miikkulainen (2024); Nguyen et al. (2025), we measure the ability of each uncertainty score to separate correct from incorrect greedy generations using Area Under the ROC Curve (AUC, %). A generation is deemed correct if it satisfies an exact match on reasoning tasks (Arithmetics, SVAMP) or achieves an ROUGE-L F1 score (Lin, 2004) greater than 0.3 on QA tasks (SciQ, GPQA), consistent with prior work.

Sampling and Implementation We sample $N=10$ completions per question using multinomial sampling at temperature $\tau=1$ via vLLM (Kwon et al., 2023). All sampling-based baselines use these same $N=10$ generations (except ANLL/NLL, which use only the greedy output). For self-consistency, uncertainty is computed as $1 - \text{count of majority answer}/N$. For all baselines, we use the suggested hyperparameters following their original setup (PRO: $\alpha = 0.4$, CE: $p = 0.3$). Our RDS variants and EigenEmbed use the widely adopted all-MiniLM-L6-v2 sentence transformer (Reimers and Gurevych, 2019). All experiments run on a single H100-80GB GPU.

5.2 Hallucination Detection Performance

Table 1 summarizes AUC performance across all 16 model–dataset pairs.

Our methods consistently outperform all baselines across all settings. On average, RDS_w achieves the highest AUC of 79.7%, followed by RDS and RDS_{ℓ_2} at 78.9% and 78.2%, surpassing the next best (EE) by a clear margin of 2.1, 1.3, and 0.6%, respectively. The stable superiority of ℓ_1 -based variants (RDS and RDS_w) over their ℓ_2 counterpart (RDS_{ℓ_2}), especially on Arithmetics, further validates our design choice, fully consistent with the rationale in Section 4.1. Notably, RDS_w ranks first in 10 out of 16 settings, demonstrating remarkable robustness across diverse tasks and model architectures.

The superiority of our scores is particularly pronounced on mathematical datasets (Arithmetic and SVAMP), where the gap over EE widens to 3–5% in several cases. This aligns with our theoretical analysis in Section 4.2: when generated answers exhibit high lexical diversity (common in free-form

Table 1: AUC performance comparison across datasets and models. All values are reported in percentages. Best scores are bolded, second-best values are underlined. RDS_{ℓ_2} denotes our base metric computed using ℓ_2 -norm (Eq. (8)), included for reference. Our metrics (RDS_{ℓ_2} , RDS , and RDS_w) are highlighted with shaded backgrounds. ES is unavailable (–) on Gemma2 because the Gemma family does not expose hidden states.

Dataset	Model	ANLL	NLL	PRO	SE	Deg	SD	SC	ES	EE	RDS_{ℓ_2}	RDS	RDS_w
GPQA	Falcon3	72.5	62.2	60.2	50.4	66.3	65.3	51.6	64.9	65.6	66.5	<u>67.5</u>	67.0
	Gemma2	62.6	63.6	65.2	50.5	63.2	61.9	51.6	–	63.0	62.5	63.0	<u>63.7</u>
	Llama3.1	64.1	64.1	59.4	53.3	59.0	58.2	51.6	63.3	62.4	<u>64.7</u>	64.4	66.0
	Llama3.2	57.2	57.2	63.8	48.2	56.4	54.9	59.8	56.8	63.9	<u>64.5</u>	64.3	67.1
SciQ	Falcon3	60.0	57.5	62.1	57.0	70.2	69.4	69.1	62.4	73.2	72.9	<u>73.4</u>	74.2
	Gemma2	59.9	59.3	68.2	59.0	72.5	72.4	74.0	–	74.1	75.1	75.4	<u>75.2</u>
	Llama3.1	64.4	64.4	57.6	63.7	75.2	73.8	76.5	56.4	77.0	77.8	<u>78.4</u>	78.8
	Llama3.2	64.2	64.2	54.5	65.1	72.5	71.0	73.2	59.1	73.2	75.0	<u>75.1</u>	75.3
Arithmetics	Falcon3	70.0	76.7	77.0	83.3	89.9	<u>89.7</u>	85.4	85.7	83.6	83.3	85.3	86.6
	Gemma2	49.6	49.6	56.4	83.4	84.7	84.1	83.2	–	82.6	84.7	<u>85.1</u>	86.3
	Llama3.1	71.3	71.3	56.8	84.7	87.5	87.9	86.3	64.4	83.6	85.4	88.7	<u>88.4</u>
	Llama3.2	71.2	71.2	67.7	87.9	87.8	87.9	<u>88.8</u>	58.4	87.6	87.2	87.9	89.0
SVAMP	Falcon3	91.7	91.7	92.3	89.2	90.9	93.0	94.4	66.6	93.4	94.0	<u>94.7</u>	95.1
	Gemma2	53.3	47.5	69.1	75.3	83.2	83.8	<u>84.9</u>	–	82.8	82.9	83.7	85.0
	Llama3.1	57.9	57.9	68.9	84.3	86.7	87.8	92.4	64.4	90.4	90.2	90.6	<u>91.4</u>
	Llama3.2	62.1	62.1	57.7	80.3	80.0	79.3	<u>86.2</u>	60.8	84.8	84.4	84.6	86.4
Average		64.5	63.8	64.8	69.7	76.6	76.3	75.6	63.6	77.6	78.2	<u>78.9</u>	79.7
Best Count		1	0	1	0	1	0	1	0	0	0	2	10

math solutions, where responses differing by even a single character or magnitude, e.g., “1” vs. “10”, are semantically distant, the proposed RDS metric better captures the underlying semantic clustering than eigenvector-based methods.

Self-Consistency (SC) performs strongly on math problems (frequently ranking in the top-3 on Arithmetics and SVAMP), but its effectiveness drops considerably on datasets where exact-match evaluation is not applicable (GPQA and SciQ). This confirms that SC remains highly dependent on the availability of a verifiable, correct answer. Other baselines, such as SD and Deg show competitive results on specific tasks (mostly QA), but show limited performance on mathematics datasets. Simple probability-based methods (NLL, ALL) generally lag behind, underscoring the importance of modeling response similarity in the embedding space.

Overall, the proposed RDS and weighted variant RDS_w maintain robustness across model families and dataset characteristics.

5.3 Best-Of- N Ranking Performance

Table 2 reports accuracy when methods are used to rank multiple generations per question and select the least-uncertain answer. Among these, RDS^s and its weighted variant achieve the highest average accuracy, outperforming the second-best (CE)

Table 2: Best-of- N selection accuracy (%) using per-sample uncertainty scores (lower uncertainty score indicates better sample). Our metrics (RDS^s and RDS_w^s) are highlighted with shaded backgrounds.

Dataset	Model	ANLL	NLL	SC	CE	RDS^s	RDS_w^s
GPQA	Falcon3	28.0	24.4	22.8	22.8	26.4	28.5
	Gemma2	23.8	20.7	19.2	19.2	24.4	25.9
	Llama3.1	20.7	20.2	17.6	18.1	23.8	26.4
	Llama3.2	19.7	20.2	16.6	22.8	22.8	23.8
SciQ	Falcon3	64.3	66.8	67.8	67.8	68.3	67.3
	Gemma2	73.0	74.0	74.6	74.4	75.1	74.9
	Llama3.1	62.2	62.7	67.6	67.7	67.5	68.0
	Llama3.2	52.8	53.5	59.0	59.7	60.0	58.9
Arithmetics	Falcon3	94.6	94.6	95.0	95.0	95.0	95.0
	Gemma2	97.8	97.9	98.0	98.0	98.0	98.0
	Llama3.1	94.3	94.6	94.3	94.4	94.2	94.2
	Llama3.2	87.4	87.0	88.0	87.4	88.2	88.1
SVAMP	Falcon3	62.0	61.4	63.1	61.7	63.1	63.1
	Gemma2	72.5	71.9	72.2	72.5	72.5	72.9
	Llama3.1	65.1	65.4	68.0	68.1	67.5	67.8
	Llama3.2	52.2	53.2	60.3	59.7	58.0	58.0
Average		60.7	60.5	61.5	61.8	62.8	63.2
Best Count		0	1	4	3	7	9

by 1.4% and 1.0%, respectively. The advantage is especially striking on the high-difficulty GPQA dataset, where RDS_w achieves gains of up to 8.3% over CE and 8.8% over SC on Llama3.1-8B, while outperforming ANLL and NLL by 6.2% and 5.7%, respectively. These results further confirm the robustness of our metrics in leveraging both probability and semantic signals, and underscore the

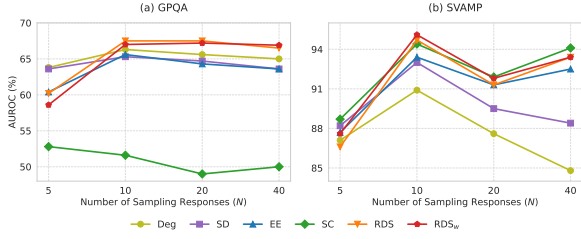


Figure 2: Ablation on the number of sampled responses N for hallucination detection across datasets. Only top baselines are selected for illustration. Detailed results of all methods are provided in Appendix A.3.

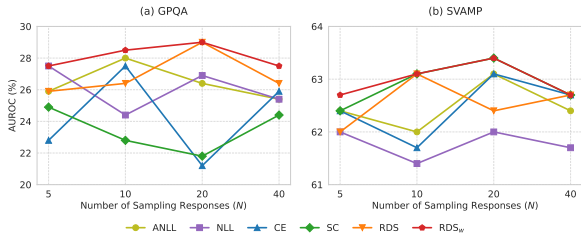


Figure 3: Ablation on the number of sampled responses for best-of- N ; see Appendix A.3 for details.

limitations of purely probability- or consistency-based methods such as SC and CE, especially on non-mathematical datasets.

5.4 Ablation Study

In this section, we investigate the effects of hyperparameters, including the number of sampling responses N and choice of embedding model E . To reduce computational overhead, we use Falcon3-7B for experiments over two representative datasets: GPQA and SVAMP.

Effect of the Number of Sampling Responses

We vary $N \in \{5, 10, 20, 40\}$ using Falcon3-7B on GPQA and SVAMP for hallucination detection and best-of- N tasks (Figures 2 and 3). For hallucination detection, on GPQA, most semantic baselines (Deg, SD, EE) peak at $N = 10$ and degrade as N increases, suggesting that additional low-probability samples introduce noise. Self-consistency (SC) performs near random (approximately 50%) at large N , as majority voting fails without a clearly dominant answer. In contrast, RDS-based methods remain robust: RDS_w shows essentially no degradation and achieves the highest AUC even at $N = 40$. On SVAMP, similar trends are observed, though variance is smaller and SC remains stable at high N , as correct mathematical solutions are often repeated verbatim. For best-of- N (Figure 3), RDS and RDS_w again demon-

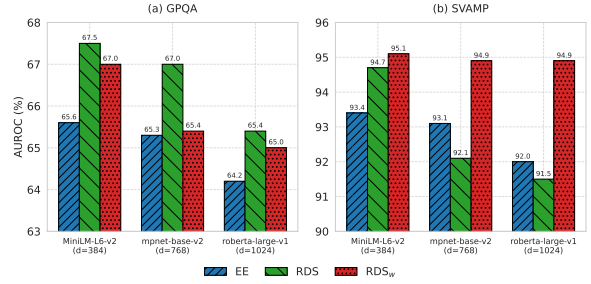


Figure 4: Effect of the sentence embedding model on hallucination detection across (a) GPQA and (b) SVAMP using $N=10$.

strate strong consistency across sampling budgets, particularly on GPQA, while baselines degrade or fluctuate at large N . Overall, RDS-based metrics are uniquely tolerant to noisy generations, making them well-suited to large sampling budgets.

Effect Of Embedding Models

In Figure 4, we compare three sentence transformers of increasing capacity: all-miniLM-L6-v2 (384-d, our default), all-mpnet-base-v2 (768-d), and all-roberta-large-v1 (1024-d). On GPQA, all methods (EE, RDS, and RDS_w) degrade slightly (1.4–2.1%) with larger encoders, consistent with observations that larger contrastively trained sentence transformers can exhibit embedding space anisotropy and representation biases, where certain semantic dimensions dominate the embeddings, leading to suboptimal performance on specialized QA domains (Nikolaev and Padó, 2023). In contrast, RDS_w remains highly stable on SVAMP, with AUC varying by at most $\pm 0.2\%$. Overall, these results indicate that incorporating generation probabilities reduces sensitivity to encoder choice while preserving most performance of the lightweight default model.

6 Conclusion

We propose Radial Dispersion Score (RDS), a simple, training-free, model-agnostic uncertainty estimator that measures radial dispersion of sampled generations, with an optional probability-weighted variant. RDS naturally extends to strong per-sample uncertainty estimates that complement probability- and consistency-based methods while remaining lightweight. Across four QA datasets and four LLMs, RDS achieves state-of-the-art hallucination detection and best-of- N performance, demonstrating robustness and scalability with respect to sample size and embedding choice.

Limitations

RDS requires an external sentence encoder. While a lightweight encoder delivers excellent performance and probability weighting reduces dependence on the specific encoder, heavier models can still introduce modest degradation on difficult tasks such as GPQA. In scenarios where any external embedder is undesirable, purely probability-based alternatives remain the only option. Like all sampling-based methods, RDS requires generating multiple completions per input, though robust results are achieved with moderate sampling budgets.

References

- Lukas Aichberger, Kajetan Schweighofer, and Sepp Hochreiter. 2024. Rethinking uncertainty estimation in natural language generation. *arXiv preprint arXiv:2412.15176*.
- Ebtesam Almazrouei, Hamza Alobeidli, Abdulaziz Alshamsi, Alessandro Cappelli, Ruxandra Cojocaru, M erouane Debbah,  tienne Goffinet, Daniel Hesslow, Julien Launay, Quentin Malartic, and 1 others. 2023. The falcon series of open language models. *arXiv preprint arXiv:2311.16867*.
- Tom Brown, Benjamin Mann, Nick Ryder, Melanie Subbiah, Jared D Kaplan, Prafulla Dhariwal, Arvind Neelakantan, Pranav Shyam, Girish Sastry, Amanda Askell, and 1 others. 2020. Language models are few-shot learners. *Advances in neural information processing systems*, 33:1877–1901.
- Chao Chen, Kai Liu, Ze Chen, Yi Gu, Yue Wu, Mingyuan Tao, Zhihang Fu, and Jieping Ye. 2024. Inside: LLMs’ internal states retain the power of hallucination detection. *arXiv preprint arXiv:2402.03744*.
- Xinyun Chen, Renat Aksitov, Uri Alon, Jie Ren, Kefan Xiao, Pengcheng Yin, Sushant Prakash, Charles Sutton, Xuezhi Wang, and Denny Zhou. 2023. Universal self-consistency for large language model generation. *arXiv preprint arXiv:2311.17311*.
- Sebastian Farquhar, Jannik Kossen, Lorenz Kuhn, and Yarin Gal. 2024. Detecting hallucinations in large language models using semantic entropy. *Nature*, 630(8017):625–630.
- Shiqi Gao, Tianxiang Gong, Zijie Lin, Runhua Xu, Haoyi Zhou, and Jianxin Li. 2025. [Flue: Streamlined uncertainty estimation for large language models](#). *Proceedings of the AAAI Conference on Artificial Intelligence*, 39(16):16745–16753.
- Aaron Grattafiori, Abhimanyu Dubey, Abhinav Jauhri, Abhinav Pandey, Abhishek Kadian, Ahmad Al-Dahle, Aiesha Letman, Akhil Mathur, Alan Schelten, Alex Vaughan, and 1 others. 2024. The llama 3 herd of models. *arXiv preprint arXiv:2407.21783*.
- Nuno M Guerreiro, Elena Voita, and Andr e FT Martins. 2023. Looking for a needle in a haystack: A comprehensive study of hallucinations in neural machine translation. In *Proceedings of the 17th Conference of the European Chapter of the Association for Computational Linguistics*, pages 1059–1075.
- Trevor Hastie, Robert Tibshirani, Jerome Friedman, and James Franklin. 2005. The elements of statistical learning: data mining, inference and prediction. *The Mathematical Intelligencer*, 27(2):83–85.
- Bairu Hou, Yujian Liu, Kaizhi Qian, Jacob Andreas, Shiyu Chang, and Yang Zhang. 2024. Decomposing uncertainty for large language models through input clarification ensembling. In *International Conference on Machine Learning*, pages 19023–19042. PMLR.
- Lei Huang, Weijiang Yu, Weitao Ma, Weihong Zhong, Zhangyin Feng, Haotian Wang, Qianglong Chen, Weihua Peng, Xiaocheng Feng, Bing Qin, and 1 others. 2025. A survey on hallucination in large language models: Principles, taxonomy, challenges, and open questions. *ACM Transactions on Information Systems*, 43(2):1–55.
- Ziwei Ji, Nayeon Lee, Rita Frieske, Tiezheng Yu, Dan Su, Yan Xu, Etsuko Ishii, Ye Jin Bang, Andrea Madotto, and Pascale Fung. 2023. Survey of hallucination in natural language generation. *ACM computing surveys*, 55(12):1–38.
- Saurav Kadavath, Tom Conerly, Amanda Askell, Tom Henighan, Dawn Drain, Ethan Perez, Nicholas Schiefer, Zac Hatfield-Dodds, Nova DasSarma, Eli Tran-Johnson, and 1 others. 2022. Language models (mostly) know what they know. *arXiv preprint arXiv:2207.05221*.
- Zhewei Kang, Xuandong Zhao, and Dawn Song. 2025. Scalable best-of-n selection for large language models via self-certainty. *arXiv preprint arXiv:2502.18581*.
- Maya Kruse, Majid Afshar, Saksham Khatwani, Anoop Mayampurath, Guanhua Chen, and Yanjun Gao. 2025. Simple yet effective: An information-theoretic approach to multi-LLM uncertainty quantification. In *Proceedings of the 2025 Conference on Empirical Methods in Natural Language Processing*, pages 30481–30492.
- Lorenz Kuhn, Yarin Gal, and Sebastian Farquhar. 2023a. Semantic uncertainty: Linguistic invariances for uncertainty estimation in natural language generation. In *The Eleventh International Conference on Learning Representations*.
- Lorenz Kuhn, Yarin Gal, and Sebastian Farquhar. 2023b. Semantic uncertainty: Linguistic invariances for uncertainty estimation in natural language generation. In *NeurIPS ML Safety Workshop*.
- Woosuk Kwon, Zhuohan Li, Siyuan Zhuang, Ying Sheng, Lianmin Zheng, Cody Hao Yu, Joseph E.

- Gonzalez, Hao Zhang, and Ion Stoica. 2023. Efficient memory management for large language model serving with pagedattention. In *Proceedings of the ACM SIGOPS 29th Symposium on Operating Systems Principles*.
- Chin-Yew Lin. 2004. Rouge: A package for automatic evaluation of summaries. In *Text summarization branches out*, pages 74–81.
- Zhen Lin, Shubhendu Trivedi, and Jimeng Sun. 2023. Generating with confidence: Uncertainty quantification for black-box large language models. *arXiv preprint arXiv:2305.19187*.
- Andrey Malinin and Mark Gales. 2021. Uncertainty estimation in autoregressive structured prediction. In *International Conference on Learning Representations*.
- Potsawee Manakul, Adian Liusie, and Mark Gales. 2023. Selfcheckgpt: Zero-resource black-box hallucination detection for generative large language models. In *Proceedings of the 2023 Conference on Empirical Methods in Natural Language Processing*, pages 9004–9017.
- Thomas Mesnard, Cassidy Hardin, Robert Dadashi, Surya Bhupatiraju, Shreya Pathak, Laurent Sifre, Morgane Rivière, Mihir Sanjay Kale, Juliette Love, and 1 others. 2024. Gemma: Open models based on gemini research and technology. *arXiv preprint arXiv:2403.08295*.
- Manh Nguyen, Sunil Gupta, and Hung Le. 2025. Probabilities are all you need: A probability-only approach to uncertainty estimation in large language models. *arXiv preprint arXiv:2511.07694*.
- Alexander Nikitin, Jannik Kossen, Yarin Gal, and Pekka Marttinen. 2024. Kernel language entropy: Fine-grained uncertainty quantification for llms from semantic similarities. *Advances in Neural Information Processing Systems*, 37:8901–8929.
- Dmitry Nikolaev and Sebastian Padó. 2023. **Representation biases in sentence transformers**. In *Proceedings of the 17th Conference of the European Chapter of the Association for Computational Linguistics*, pages 3701–3716, Dubrovnik, Croatia. Association for Computational Linguistics.
- Arkil Patel, Satwik Bhattamishra, and Navin Goyal. 2021. Are nlp models really able to solve simple math word problems? In *Proceedings of the 2021 Conference of the North American Chapter of the Association for Computational Linguistics: Human Language Technologies*, pages 2080–2094.
- Gabriel Peyré, Marco Cuturi, and 1 others. 2019. Computational optimal transport: With applications to data science. *Foundations and Trends® in Machine Learning*, 11(5-6):355–607.
- Edward Phillips, Sean Wu, Soheila Molaei, Danielle Belgrave, Anshul Thakur, and David Clifton. 2025. Geometric uncertainty for detecting and correcting hallucinations in llms. *arXiv preprint arXiv:2509.13813*.
- Xin Qiu and Risto Miikkulainen. 2024. Semantic density: Uncertainty quantification for large language models through confidence measurement in semantic space. In *The Thirty-eighth Annual Conference on Neural Information Processing Systems*.
- Nils Reimers and Iryna Gurevych. 2019. Sentence-bert: Sentence embeddings using siamese bert-networks. *arXiv preprint arXiv:1908.10084*.
- David Rein, Betty Li Hou, Asa Cooper Stickland, Jackson Petty, Richard Yuanzhe Pang, Julien Dirani, Julian Michael, and Samuel R Bowman. 2024. Gpqa: A graduate-level google-proof q&a benchmark. In *First Conference on Language Modeling*.
- Filippo Santambrogio. 2015. Optimal transport for applied mathematicians.
- Xinglin Wang, Yiwei Li, Shaoxiong Feng, Peiwen Yuan, Boyuan Pan, Heda Wang, Yao Hu, and Kan Li. 2024. Integrate the essence and eliminate the dross: Fine-grained self-consistency for free-form language generation. In *Proceedings of the 62nd Annual Meeting of the Association for Computational Linguistics (Volume 1: Long Papers)*, pages 11782–11794.
- Xuezhi Wang, Jason Wei, Dale Schuurmans, Quoc Le, Ed Chi, Sharan Narang, Aakanksha Chowdhery, and Denny Zhou. 2022. Self-consistency improves chain of thought reasoning in language models. *arXiv preprint arXiv:2203.11171*.
- Johannes Welbl, Nelson F Liu, and Matt Gardner. 2017. Crowdsourcing multiple choice science questions. *arXiv preprint arXiv:1707.06209*.
- Zhanghao Zhouyin and Ding Liu. 2021. Understanding neural networks with logarithm determinant entropy estimator. *arXiv preprint arXiv:2105.03705*.

A Appendix

A.1 Proof of Proposition 1

Proof. Let $\mathbf{v}_i = \mathbf{u}_i - \bar{\mathbf{u}}$ denote the centered embeddings.

Step 1: EigenEmbed bounds We first compute the squared ℓ_2 norms of the centered embeddings:

$$\sum_{i=1}^N \|\mathbf{v}_i\|_2^2 = \sum_{i=1}^N \|\mathbf{u}_i - \bar{\mathbf{u}}\|_2^2 \quad (13)$$

$$= \sum_{i=1}^N (\|\mathbf{u}_i\|_2^2 - 2\mathbf{u}_i^\top \bar{\mathbf{u}} + \|\bar{\mathbf{u}}\|_2^2). \quad (14)$$

Since $\|\mathbf{u}_i\|_2^2 = 1$ and $\sum_i \mathbf{u}_i = N\bar{\mathbf{u}}$, the middle term simplifies, yielding

$$\sum_{i=1}^N \|\mathbf{v}_i\|_2^2 = N - 2N\|\bar{\mathbf{u}}\|_2^2 + N\|\bar{\mathbf{u}}\|_2^2 = N(1 - \|\bar{\mathbf{u}}\|_2^2).$$

Hence, by definition,

$$\text{EigenEmbed} = \frac{1}{N} \sum_{i=1}^N \|\mathbf{v}_i\|_2^2 = 1 - \|\bar{\mathbf{u}}\|_2^2 \in [0, 1].$$

Step 2: RDS lower bound By definition, the ℓ_1 norm of each centered embedding is non-negative: $\|\mathbf{v}_i\|_1 \geq 0$ for all i , which implies

$$\sum_{i=1}^N \|\mathbf{v}_i\|_1 \geq \sqrt{\sum_{i=1}^N \|\mathbf{v}_i\|_2^2}. \quad (15)$$

We can rewrite the right-hand side in terms of EigenEmbed:

$$\text{RDS} = \sum_{i=1}^N \|\mathbf{v}_i\|_1 \quad (16)$$

$$\geq \sqrt{\sum_{i=1}^N \|\mathbf{v}_i\|_2^2} \quad (17)$$

$$= \sqrt{N \cdot \text{EigenEmbed}} \quad (18)$$

$$\geq \sqrt{N} \cdot \text{EigenEmbed} \quad (19)$$

$$\geq \text{EigenEmbed}. \quad (20)$$

Eq. (19) and Eq. (20) uses the fact that $\text{EigenEmbed} \in [0, 1]$ (step 1) and $N > 1$, respectively. \square

Equality conditions Equality in Eq. (15) occurs if and only if all centered embeddings $\mathbf{v}_i = \mathbf{0} \forall i$, this corresponds to all original embeddings \mathbf{u}_i being identical. The final inequality $\sqrt{N \cdot \text{EigenEmbed}} \geq \text{EigenEmbed}$ is strict for $N > 1$, which ensures that $\text{RDS} > \text{EigenEmbed}$ unless the embeddings are identical ($\text{EigenEmbed} = 0$). Intuitively, the gap between RDS and EigenEmbed grows as the mean embedding $\bar{\mathbf{u}} \rightarrow \mathbf{0}$, reflecting greater dispersion among the embeddings.

A.2 Proof of Proposition 2

Proof. Compute the squared norm of the total sum:

$$\left\| \sum_{i=1}^N \mathbf{u}_i \right\|_2^2 = \sum_{i=1}^N \sum_{j=1}^N \mathbf{u}_i^\top \mathbf{u}_j.$$

If $\bar{\mathbf{u}} = \mathbf{0}$, then $\sum_i \mathbf{u}_i = \mathbf{0}$ and the left-hand side is zero. Expanding the double sum separates diagonal and off-diagonal terms:

$$0 = \sum_{i=1}^N \|\mathbf{u}_i\|_2^2 + \sum_{i \neq j} \mathbf{u}_i^\top \mathbf{u}_j = N + \sum_{i \neq j} \mathbf{u}_i^\top \mathbf{u}_j.$$

Hence $\sum_{i \neq j} \mathbf{u}_i^\top \mathbf{u}_j = -N$, and dividing by the $N(N-1)$ off-diagonal entries gives the stated average:

$$\frac{1}{N(N-1)} \sum_{i \neq j} \mathbf{u}_i^\top \mathbf{u}_j = -\frac{1}{N-1} < 0.$$

If for some fixed i we had $\mathbf{u}_i^\top \mathbf{u}_j \geq 0$ for all $j \neq i$, then summing would give

$$\mathbf{u}_i^\top \left(\sum_{j \neq i} \mathbf{u}_j \right) \geq 0.$$

But $\sum_{j \neq i} \mathbf{u}_j = -\mathbf{u}_i$ (since the total sum is zero), so the left-hand side equals $-\|\mathbf{u}_i\|_2^2 = -1$, a contradiction. Thus every i has at least one j with $\mathbf{u}_i^\top \mathbf{u}_j < 0$. \square

A.3 Extended Results: Number Of Samples

Table 3: Full hallucination detection performance on GPQA and SVAMP using Falcon3-7B across different number of sampling responses.

N	PRO	SE	Deg	SD	ES	EE	SC	RDS	RDS _w
GPQA									
5	0.547	0.513	0.638	0.636	0.606	0.604	0.528	0.602	0.586
10	0.602	0.504	0.663	0.653	0.649	0.662	0.516	0.675	0.670
20	0.612	0.531	0.656	0.647	0.653	0.643	0.490	0.675	0.672
40	0.603	0.525	0.650	0.636	0.669	0.636	0.500	0.665	0.669
SVAMP									
5	0.918	0.845	0.871	0.882	0.636	0.877	0.887	0.866	0.876
10	0.923	0.892	0.909	0.930	0.666	0.942	0.944	0.947	0.951
20	0.921	0.862	0.876	0.895	0.693	0.913	0.919	0.913	0.918
40	0.920	0.817	0.848	0.884	0.693	0.925	0.941	0.934	0.934

A.4 Model And Data Appendix

We list the links to the LLMs and datasets in Table 5.

Table 4: Best-of- N performance on GPQA and SVAMP using Falcon3-7B across different number of sampling responses.

N	ALL	NLL	SC	CE	RDS	RDS _w
GPQA						
5	0.259	0.275	0.249	0.228	0.259	0.275
10	0.280	0.244	0.228	0.275	0.264	0.285
20	0.264	0.269	0.218	0.212	0.290	0.290
40	0.254	0.254	0.244	0.259	0.264	0.275
SVAMP						
5	0.624	0.620	0.624	0.624	0.620	0.627
10	0.620	0.614	0.631	0.617	0.631	0.631
20	0.631	0.620	0.634	0.631	0.634	0.634
40	0.624	0.617	0.627	0.627	0.627	0.627

Models/Datasets	URL
Falcon3-7B	https://huggingface.co/tiiuae/Falcon3-7B-Instruct
Gemma2-9B	https://huggingface.co/google/gemma-2-9b-it
Llama3.1-8B	https://huggingface.co/meta-llama/Llama-3.1-8B-Instruct
Llama3.2-3B	https://huggingface.co/meta-llama/Llama-3.2-3B-Instruct
SciQ	https://github.com/launchlpl/LitCab/blob/main/sciq/test.txt
GPQA	https://huggingface.co/datasets/Idavidrein/gpqa
Arithematics	https://huggingface.co/datasets/EleutherAI/arithmetic/resolve/main/data/single_digit_three_ops.jsonl
SVAMP	https://huggingface.co/datasets/ChilleD/SVAMP

Table 5: Models and Datasets Details.